Journal of Scientific Research and Advances

Elastic and mechanical properties of high purity Na-Ca-P-B:Cu glasses–quenching route

S. Shailajha[a*], K. Geetha[a], P. Vasantharani[b]

Cite this article: J. Sci. Res. Adv. Vol. 2, No. 3, 2015, 108-114.

Glasses in the system Na_2O-CaO-B_2O_3-P_2O_5-CuO with different CuO contents have been prepared by melt quenching technique. X-ray diffraction, Pulse echo analysis and Vickers hardness analysis were investigated. The amorphous and few crystalline nature of these samples was verified by XRD. Elastic properties, Poisson's ratio, micro-hardness and Debye temperature were assessed by sound wave velocity measurements. The results showed that, density increases, the molar volume decreases as both the ultrasonic velocity and the transition temperature increases with increasing the concentration of CuO. Elastic properties studies on the network structure of these glass samples, have revealed that Cu^+/Cu^{2+} ions are incorporated in the form of CuO, decreasing the molar volume and compensate for the decrease in the average coordination number of boron atoms which was the reason for the increase in elastic moduli. Hardness was analysed by Vickers hardness tester. The results showed that the mechanical strength of the glass was increased with the increase of CuO content.

ISSN 2395-0226

Introduction

Newly glassy materials from alkali borate glasses with high ionic conductivity are receiving considerable attention because of their unique properties and their potential applications[1-4]. Alkali borate glasses show the anomalous composition dependences of physical properties, such as density, sound velocity and thermal expansion by the addition of alkali oxide to pure B_2O_3 glass[5]. In these glasses two group of bands, one due to the trigonal BO_3 and the second due to the tetragonal BO_4 units are present. Borate glasses are also interesting as inorganic hosts for transition metal ions.

Phosphate glasses have recently been considered for many applications due to a series of attractive properties such as low glass transition and melting temperatures, high thermal expansion coefficient, biocompatibility, low dispersion and high refractive indices, which recommend them in many applications such as, photonics, fast ion conductors[6-9] and glass to metal seals[10-12], self cleaning ability for NH_3 gas adsorption and most recently biomedical engineering. Previous studied have clarified that these applications require the optimization of phosphate based glasses property that is achievable by tuning their composition and structure.

Na_2O causes a reduction in the melting point and facilitate the homogenization of the glass system, thereby decreasing the possible structural defects[13]. The role of Na_2O in the B_2O_3 network is to modify the host structure through the transformation of the structural units of the borate network from [BO_3] to [BO_4].

Sodium Diborate is a type of glasses that consists of one-third of sodium oxide and two-third of boron oxide. This type of borate glasses draws great attention due to their improved electrical and optical properties when modified by phthalocyanine or by rare earth ions. The presence of P_2O_5 in the matrix of alkali borate glasses improves the glass quality and enhances the IR transmission, especially when modified the rare earth ions. Furthermore, borophosphate glasses possess a variety of other useful parameters. The combination of two glass formers P_2O_5 and B_2O_3 is an intrinsically interesting subject of study. The properties of the mixed glasses are specific to the mixture, being distinct from the properties of either pure or phosphate networks. The basic units of pure amorphous borate glasses are trigonal BO_3 groups, whereas the basic units of pure amorphous phosphate glasses are PO_4 tetrahedra linked through covalent bridging oxygens. The addition of modifier oxide to borate and phosphate networks has differing effects. In a borate network, the addition of a modifier oxide the degree of polymerization, the boron coordination changes from trigonal to tetrahedral, and the basic units changes from BO_3 to BO_4. In the phosphate network, the addition of a modifier oxide has the opposite effect, it has a depolymerizing effect; the extra oxygen atoms introduced by the modifier oxides form negative non-bridging oxygen sites, whose charge is compensated by the positive charge of the modifier cations [14].

Copper phosphate glasses have interesting electrical conduction and optical absorption in the visible, resulting in coloration of the glass. In Addition, copper in sodium borophosphate glasses have improved chemical durability; therefore, copper contribute to the stabilization of the glass structure. From the technological importance of these glasses and their interesting properties and potential applications, it would be interesting to study the role of CuO oxides in the formation of a glass with their participation[15].

Glasses have important advantages over crystals because of their potentially higher doping levels of rare earth ions, flexible geometry and ease of fabrication. The broader spectral features in

glasses also favour energy transfer process. Our paper is a continuation of research concerning the behaviour of transition metal ions in glasses of various chemical compositions based on their optical spectra.

Ultrasonic characterization of materials is a versatile tool for the inspection of their microstructure and their mechanical properties. This is possible because of the close association of the ultrasound waves with the elastic and the inelastic properties of the materials. There have been studies and reports on several binary alkali borate glasses, which show that there is a correlation between elastic properties and borate glass structure [14].

In the present study, we study micro-hardness, longitudinal and shear sound wave velocities and their elastic properties of Na_2O-CaO-B_2O_3-P_2O_5:CuO glasses. Part of this work was published by S.Shailajha et al. in the journal of Spectrochemica Acta Part A: Molecular and Biomolecular Spectroscopy[16]. In addition, an attempt has been to do such kind of correlation between the changes in ultrasound velocities and elastic properties to the anticipated structural changes in the CuO doped borate glassy network using XRD.

Materials and methods

Experimental

All the used reagents were analytical grade and employed as received without further purification. The composition of the glass was Na_2O, CaO, P_2O_5, B_2O_3 and dopant of CuO for which the oxides composition and samples code are listed in Table 1. The starting materials were reagent grade of Na_2O, CaO, P_2O_5 and B_2O_3. Stoichiometric mixture of Na_2O, CaO, P_2O_5 and B_2O_3 were weighed and mixed thoroughly in an agate mortar with pestle for about 2 hours to get good homogeneity. The batch mixture was transferred into an Alumina crucible. The crucible was covered and heated in an electric furnace for about 6 hrs at the temperature of 930K to allow the phosphate to decompose and react with other batch constituent before melting occur, ordinarily. The glass samples were then annealed in an oven at 130 K for 2 hours to reduce thermal stresses. The glass samples were polished using diamond disc and diamond powder to produce parallel opposite surfaces for ultrasonic velocity measurements. The photograph of the glass samples is shown in Fig.1.

Methods

X-Ray diffraction analysis

The amorphous nature of the samples is confirmed by X-ray diffraction technique using Xpert-pro diffracted method operated at 40 kV voltage and 30 mA current from 10^o to 80^o utilizing CuKα radiation source (λ=1.54060 Å).

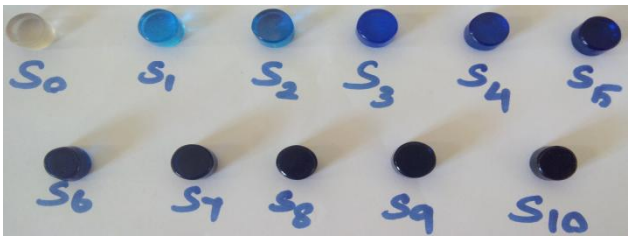

Fig. 1 Photograph of NCPBC glass samples

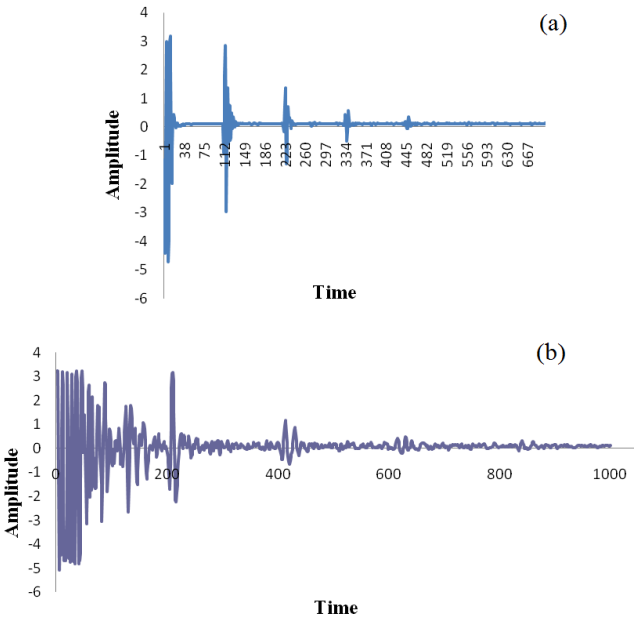

Fig. 2 Longitudinal (a) and shear (b) waveform

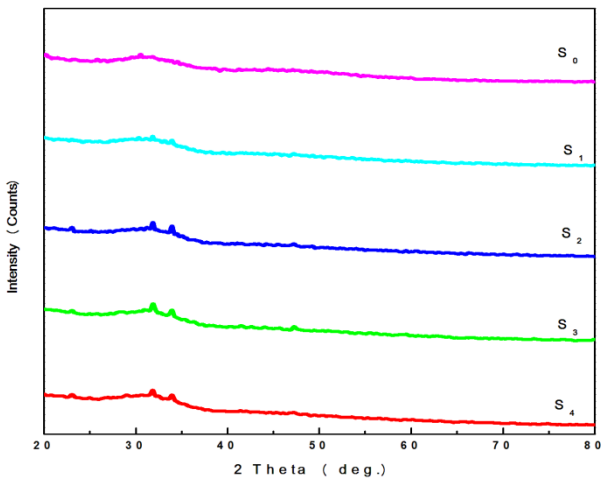

Fig. 3 XRD patterns for samples S_0 – S_4

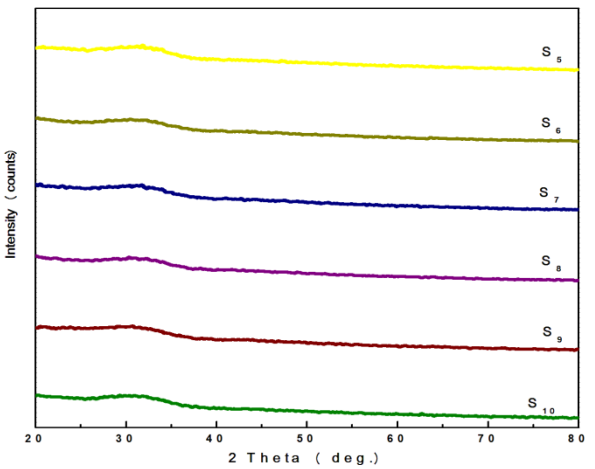

Fig. 4 XRD Patterns for Samples S_5 – S_{10}

Density measurements

The densities of the glasses were determined by Archimedes method with benzene as an immersion liquid and applying the relationship (1)

$$\rho = \frac{W_1}{(W_1 - W_2)}\rho_B \qquad (1)$$

where ρ_B is the density of the immersion liquid, and where W_1 and W_2 are the sample weights in air and in the immersion fluid, respectively. The experiments were repeated three times to obtain an accurate value of the density. The estimated error in these measurements was about ±0.001gcm^{-3}.

Ultrasonic measurements

To measure the ultrasonic velocity in the glass samples, an ultrasonic flaw detector, PANAMETRICS 5800PR was used. The ultrasonic waves were generated from a quartz transducer with a resonant frequency of 5MHz and acts as transmitter-receiver at the same time. The ultrasonic wave velocities U can be calculated by following equation,

$$U = \frac{2d}{\Delta t} \quad (\text{mms}^{-1}) \qquad (2)$$

Where d is the sample thickness (mm) and Δt is the time interval (s). The measurements were repeated three times to check the reproducibility of the data. The estimated error in the velocity measurements were ±11 ms^{-1} and ±8 ms^{-1} for longitudinal and shear velocities, respectively. Figs 2 (a) & (b) show one such echo wave form obtained for longitudinal and shear waves.

Vickers hardness measurements

The Hardness measurements have been made in the Vickers scale (H_v) with a SHIMADZU apparatus. The visualization of the pyramidal stamp has been observed by using microscope. The accuracy is 0.001 g/mm^2. From deformation fracturepatterns in Vickers indenter tests, the values of the Vickers hardness, H_v for the glasses were evaluated using the standard equation,

$$H_v = (1.854)\frac{F}{d^2} \qquad (3)$$

Where F is an applied load and d is the mean indentation diagonal for a diamond pyramid indenter.

Table 1 Composition of Glass System

Sample Code	Composition (mol%)				Dopant (CuO)
	Na_2O	CaO	B_2O_3	P_2O_5	
S_0 (Pure)	26.9	24.4	2.6	46.1	0.00
S_1	26.9	24.4	2.6	46.1	0.05
S_2	26.9	24.4	2.6	46.1	0.10
S_3	26.9	24.4	2.6	46.1	0.15
S_4	26.9	24.4	2.6	46.1	0.20
S_5	26.9	24.4	2.6	46.1	0.25
S_6	26.9	24.4	2.6	46.1	0.30
S_7	26.9	24.4	2.6	46.1	0.35
S_8	26.9	24.4	2.6	46.1	0.40
S_9	26.9	24.4	2.6	46.1	0.45
S_{10}	26.9	24.4	2.6	46.1	0.50

Calculation

The elastic strain produced by a small stress can be described by two independent elastic constants, Longitudinal modulus (L) and Shear modulus (G) [17]. Elastic moduli were calculated using the following standard relations (4) – (12) [17].

Longitudinal modulus $L = \rho U_\ell^2$ (4)

Shear modulus $G = \rho U_s^2$ (5)

Bulk modulus $K = L - \left(\frac{4}{3}\right)G$ (6)

Young's modulus $E = (1+\sigma)\,2G$ (7)

Poisson's ratio $\sigma = \left[\frac{L - 2G}{2(L - G)}\right]$ (8)

Microhardness $H = (1 - 2\sigma)\frac{E}{6(1+\sigma)}$ (9)

Acoustic impedance $Z = U_\ell \rho$ (10)

Thermal expansion coefficient $\alpha_p = 23.2(U_\ell - 0.57457)$ (11)

Debye temperature $\theta_D = \frac{h}{K}\left[\frac{9N}{4\pi V_m}\right]^{1/3} Um$ (12)

where h, K, N and U_m are the Planck's constant, the Boltzmann's constant, the Avagadro's number and the mean ultrasonic velocity of the sample respectively. The uncertainties in elastic moduli, Poisson's ratio, microhardness, acoustic impedance, thermal expansion coefficient and Debye temperature were acquired from experiments repeated three times of densities and the ultrasonic velocities. These results are shown in Table 2- 4.

(3)

Table 2 Values of Density (ρ), Longitudinal Velocity (U_ℓ), Shear Velocity (U_s)

Name of the Samples	Density ρ X 10^{-3} kg m^{-3}	Molar Volume cm^3/Mol	Ultrasonic Velocity Ums^{-1}	
			Longitudinal (U_ℓ)	Shear (U_s)
S_0 (Pure)	1.2821	51.587	5650.22	2917.07
S_1	1.3040	50.752	5527.89	2907.06
S_2	1.3152	50.351	5646.55	3056.89
S_3	1.3245	50.028	5724.29	3125.67
S_4	1.3284	49.912	5732.38	3143.96
S_5	1.3321	49.803	5864.28	3245.39
S_6	1.3399	49.541	5893.98	3265.71
S_7	1.3410	49.529	5919.24	3292.79
S_8	1.3464	49.362	5924.32	3325.60
S_9	1.3548	49.085	5985.08	3395.48
S_{10}	1.3621	48.851	6029.09	3431.58

Table 3 Values of Elastic moduli

Name of the Sample	Longitudinal Modulus L X 10^9 Nm^{-2}	Shear Modulus G X 10^9 Nm^{-2}	Bulk Modulus K X 10^9 Nm^{-2}	Young's Modulus E X 10^9 Nm^{-2}
S_0 (Pure)	40.93	10.91	26.39	28.77
S_1	39.85	11.02	25.15	28.85
S_2	41.93	12.29	25.55	31.77
S_3	43.40	12.94	26.15	33.32
S_4	43.65	13.13	26.14	33.74
S_5	45.81	14.03	27.10	35.90
S_6	46.55	14.29	27.49	36.54
S_7	46.99	14.54	27.60	37.10
S_8	47.25	14.89	27.64	37.82
S_9	48.53	15.62	27.70	39.45
S_{10}	49.51	16.04	28.13	40.43

Table 4 Values of Poisson's ratio (σ), Acoustic impedance (Z), Micro hardness (H), Thermal expansion coefficient (α_p) and Debye temperature (θ_D)

Name of the sample	(σ)	Z x 10^7 $Kgm^{-2}s^{-1}$	H x 10^9 Nm^{-2}	α_p K^{-1}	θ_D K
S_0 (Pure)	0.3183	0.724	1.32	131071.87	309.08
S_1	0.3089	0.721	1.40	128233.88	309.32
S_2	0.2927	0.743	1.70	130986.67	325.44
S_3	0.2876	0.758	1.83	132790.17	333.26
S_4	0.2849	0.761	1.88	132977.81	335.35
S_5	0.2793	0.781	2.06	136037.89	346.17
S_6	0.2785	0.790	2.11	136727.01	348.92
S_7	0.2759	0.794	2.17	137313.13	351.73
S_8	0.2700	0.798	2.28	137430.78	355.37
S_9	0.2627	0.811	2.47	138840.55	363.19
S_{10}	0.2604	0.821	2.56	139861.51	367.54

Results and discussion

XRD

The vitreous nature of the studied samples was tested by XRD. The obtained XRD pattern of Pure and CuO doped glass samples with various contents of Copper Oxide are presented in Figs. 3 & 4. For Sample S_0, no crystalline phase is observed. By adding the dopant compound of CuO, the samples S_1 to S_4, are crystalline in nature. For S_5 to S_{10}, the crystalline phase changed to the amorphous state due to increasing the dopant compound.

Density and molar volume

The values of density (ρ) and molar volume of all the glass samples have been calculated and their values are displayed in Table 2. Generally, when metal oxides are added into glass network either a decrease or an increase in density will be observed without any abnormal behaviour [18]. The density and molar volume of the glass network depend upon many factors such as structure, coordination number, cross-link density, and dimensionality of intestinal spaces. Density measurements are widely used to study the effects of composition on glass structure. These measurements are usually employed to control the homogeneity of glass, but the value of density itself is not a useful parameter. On the contrary, the determination of molar volume from density data can provide information on different aspects of the glass structure [19]. Generally, the density and the molar volume show opposite behaviour. The change in the density of the systems is related to the density of the structural units when introducing the CuO. As can be seen from the Table 2, the density increases while the molar volume decreases with increase of CuO concentration [20].

The change in density by addition of CuO is related to the change in the atomic mass and atomic volume of the constituent elements. It is clear that by increasing CuO, the molar volume decreases, which is similar to the variation density that occurs with increasing CuO content. The Cu ions may enter the glass network interstitially; hence, some network B-O-B bonds are broken and replaced by ionic bonds between Cu ions and singly bonded oxygen atoms. Therefore, if one assumed that the only effect of adding Cu cations was to break down the network B-O-B bonds, then an decrease in the molar volume with CuO content would be expected for the entire vitreous range of the studied glass system. The addition of CuO increased the values of density, which is most likely attributable to simultaneous filling up of vacancies in the network by the interstitial Cu ions with an atomic mass of 63.546. This increase in density indicates the structural changes in the glass network, which is accompanied by decrease in the molar volume [21].

Ultrasonic velocities and elastic moduli

The values of longitudinal and shear ultrasonic wave velocities for all the samples are listed in Table 2 and are graphically presented in Fig.5. The addition of CuO in glass interstices causes more ions fill up the network, thus compacting the glass structure. As a consequence, both longitudinal (U_l) and shear velocity (U_s) increase linearly with increase in mol% of doped CuO in NCPBC glass system, but the rate of increase of U_l is greater than that of U_s. The increase in ultrasonic velocity (both longitudinal and shear) is attributed to an increase in packing density because of the transformation of coordination. Due to this increase in packing density, the rigidity of the glass system increases and hence ultrasonic velocities and elastic constants. In this NCPBC glass system, CuO plays a role of a network modifier. It will modify the glass structure, thus causing the glass to become harder. Although the glass is harder, this does not mean that the glass is dense [21].

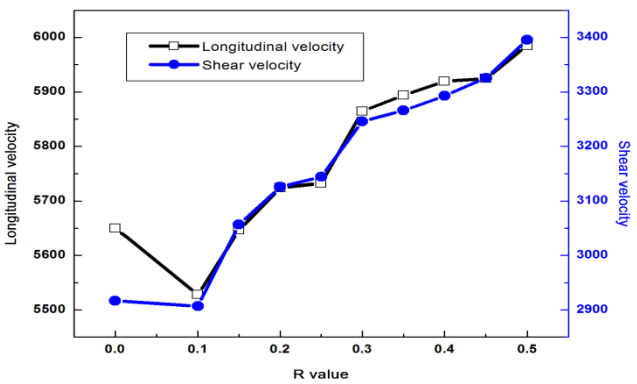

Fig. 5 Longitudinal & Shear velocity Vs Mole Fraction

The independent elastic constants for isotropic solids and glasses are the longitudinal modulus (L) and shear modulus (G). The calculation of other elastic constants and Poisson's ratio (σ) depends on the values of the density and on both of the velocities. The sound velocities also determine Young's modulus (E), which is defined as a linear stress over the linear strain and is related to the bond strength. Additionally, the bulk modulus (K) is define as the change in volume when a force is acting upon in all directions [21].

The values of elastic moduli for all samples were calculated and listed in Table 3 and are graphically presented in Figs. 6 &7. The values of the elastic moduli increases linearly with increases in the CuO content. That is, the addition of CuO to a borate glass network , the glass structure is more closely packed [22]. The increase in K with the increasing of CuO content in borophosphate glass network confirming the increase in cross-link density and consequently increased rigidity of the glass network structure [23].

The values of Poisson's ratio (σ) for all samples were calculated and listed in Table 4 and are graphically presented in Fig. 8. According to Gaafaar, Poisson's ratio is formally defined for any structure as the ratio of lateral to longitudinal strain produced when tensile forces are applied. In solid materials, the tensile strain produced in the network is unaffected by the cross-links while the lateral strain is greatly decreased with increasing covalent bonds. Bridge and Higazy [24] have suggested a close correlation between Poisson's ratio and cross-link density which is defined as the number of bridging bonds per cation [14]. According to Rao, Poisson's ratio (σ) depends on the dimensionality of the structure and cross-link density. A three dimensional network structure (e.g., SiO_2 or GeO_2) has lower σ value than that of a two-dimensional structure (e.g., B_2O_3 or P_2O_5), since the number of bonds resisting a transverse deformation decreases in that order. Therefore, addition of CuO results in a decrease of σ due to the increase in $N_{4(B)}$ and the presence of copper atoms which consequently means the increase in dimensionality of the glass network structure [23].

The values of acoustic impedance (Z), microhardness (H), thermal expansion coefficient (α_p) & Debye temperature (Θ_D) for all samples were calculated and listed in Table 4 and are graphically presented in Figs. 9 & 10. Microhardness (H) expresses the stress required to eliminate the free volume (deformation of the network) of the glass. The H has the same attitude as the elastic moduli with increase of CuO concentration. The increasing value of H indicated the increase in rigidity of the glass system. According to Gaafaar, Debye temperature (Θ_D) plays an important role in solid materials in the determination of elastic moduli and atomic vibrations. Θ_D represents the temperature at which nearly all modes of vibration in a solid are excited and its increasing trend confirms the strong formation of glass network. The continuous increase of Θ_D also suggests the compactness in the structure leading to increase in mean sound velocity [14]. That is, the increase in Θ_D is possibly due to the charge centre coming closer than the distance required statistically to achieve a more effective coulombian interaction. Such interaction can give rise to high energy vibrational modes, thereby increasing the Θ_D [25].

The increasing values of the acoustic impedance (Z) and thermal expansion coefficient (α_p) for all strongly confirms the strengthening of the glass network [26].

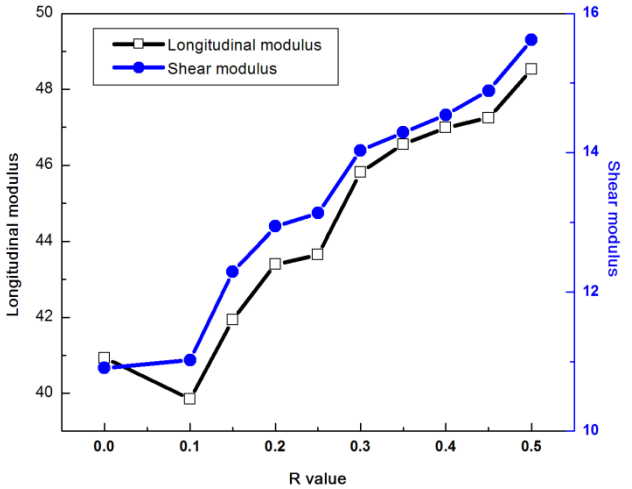

Fig. 6 Longitudinal & Shear modulus Vs Mole fraction

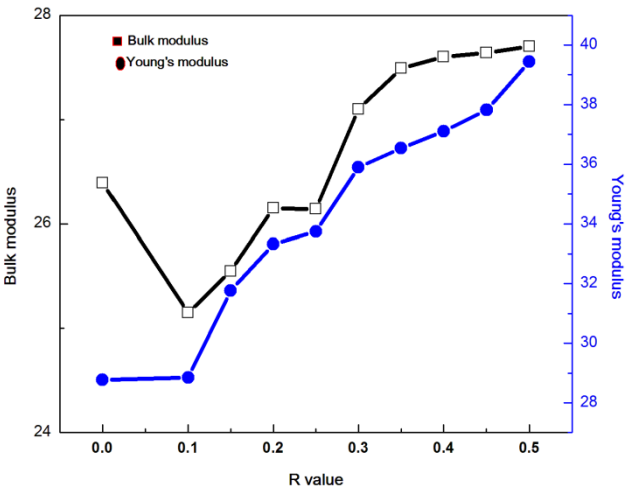

Fig. 7 Bulk & Young's modulus Vs Mole fraction

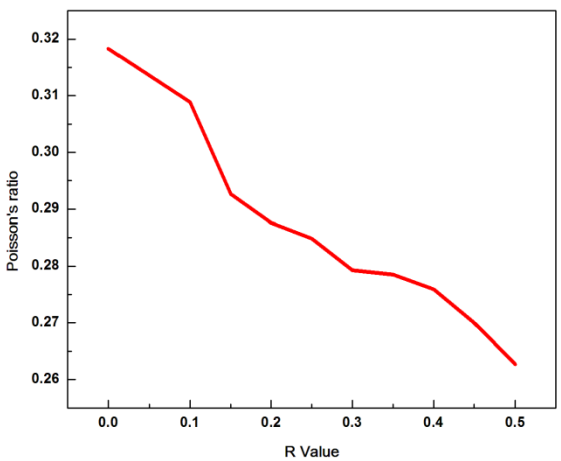

Fig. 8 Poisson's ratio Vs Mole fraction

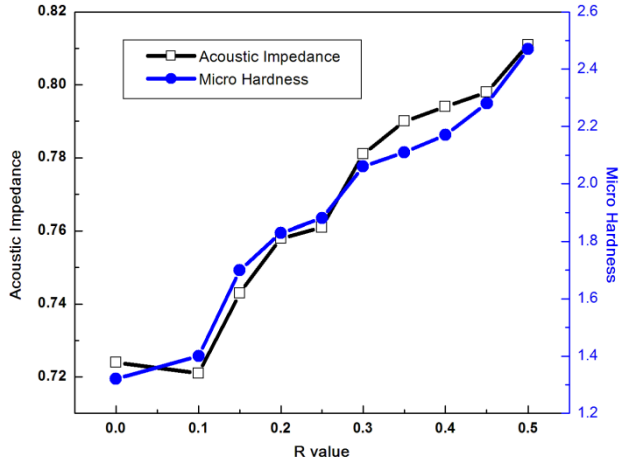

Fig. 9 Acoustic Impedance & Microhardness Vs Mole fraction

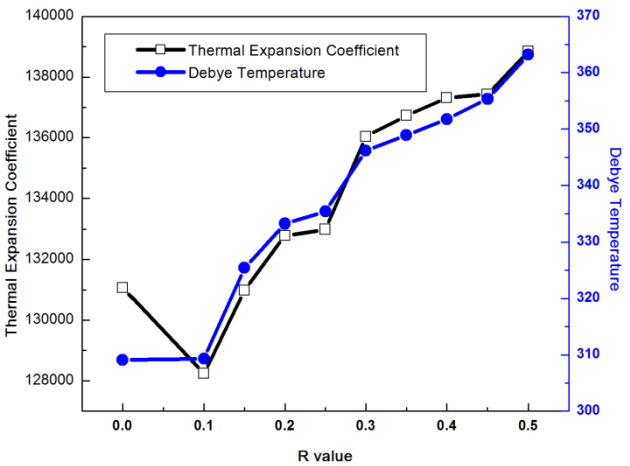

Fig. 10 Thermal expansion co-efficient & Debye Temperature Vs Mole fraction

Vickers hardness (H_v)

Hardness is observed that Vickers produced fracture patterns for the present glass were radial cracks. The evaluated values of Vickers hardness at room temperature in air are listed in the Table 5 and are also shown in Fig. 11 as a function of composition. It is seen that vickers hardness increases with increase of CuO ratio [27].

Hardness is found to increase as the load is increased and it attains a constant value for the load of 300g for pure and all doped samples. Vickers microhardness measurement show that the samples has a hardness value 342 g/mm^2 for pure, 380 g//mm^2 for 0.05 wt%, 409 g//mm^2 for 0.1 wt%, 415 g//mm^2 for 0.15 wt%, 466 g//mm^2 for 0.2 wt%, 548 g//mm^2 for 0.25 wt%, 549 g//mm^2 for 0.3 wt%, 552 g//mm^2 for 0.35 wt%, 553 g//mm^2 for 0.4 wt%, 614 g//mm^2 for 0.45 wt% and 626 g//mm^2 for 0.5 wt% of CuO doped.

Table 5 Values of Vickers hardness (H_v)

Sample	S_0	S_1	S_2	S_3	S_4	S_5	S_6	S_7	S_8	S_9	S_{10}
H_V(g/mm^2)	342	380	409	415	466	548	549	552	553	614	626

The increase in vickers hardness with increase in CuO wt% could be understood in terms of the number of bridging oxygens present in the glass. An increase in the concentration of bridging oxygens produces the connectivity of the glassy network and the elastic modulus of the glass.

Hardness increases with the average number of network constraints per atom. In other words, hardness is governed by the degree of network connectivity. Introducing alkalis into a Na_2O glass thus generally decreases H_v, whereas converting boron from three-fold to four-fold coordination in B_2O_3 glass increases [28]. From the vickers hardness studies, the mechanical strength of the sample is increased with increasing doped percentage. The increase in hardness is related to the increase of the rigidity of the glass, which further confirms the compactness structure of glass samples [29].

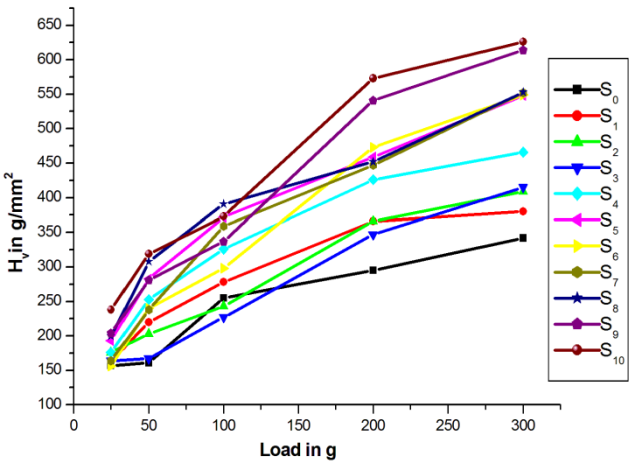

Fig. 11 Vickers hardness for Samples $S_0 - S_{10}$

Conclusion

The XRD spectra suggest that the introduction of CuO was favourable for the formation of crystalline phase. When increasing CuO, crystalline phase changed to amorphous phase. The amorphous nature was confirmed by the X-ray diffraction and change in structure of the glass matrix due to the composition effect. Our results of high ultrasonic velocity and elastic moduli reveal the high strength of the sample is mainly associated to the strong bonding between the constituent elements. The density, ultrasonic wave velocities and elastic properties have revealed that Cu^{2+} ions incorporated in the form of CuO, decreasing the molar volume and compensate for the decrease in the average coordination number of boron atoms which was the reason for the increase in elastic moduli. The increasing trend of acoustical parameters and the decreasing trend of poisson's ratio indicates that the glass system is stronger. The vickers hardness increase with increasing CuO content , indicating the increase in mechanical strength of the glass.

Acknowledgements

The authors are thankful to the UGC-SAP, New Delhi for provided the financial support and DST-FIST for provided the Analytical instrumentation facilities (XRD) to the Department of physics, Manonmaniam Sundaranar University, Tirunelveli,

Tamil Nadu, India and We acknowledge the characterization facilities provided by the NDT, IIT Madras, Chennai, India.

Notes and References

[a]*Department of Physics, Manonmaniam Sundaranar University,Tirunelveli,Tamilnadu,India*
[b]*Department of Physics, Annamalai University, Chidambaram, Tamilnadu, India*
**E-mail: drsshailajha_msu@yahoo.co*

[1] M.Balkanski, R.F.Wallis, J.Deppe, M.Masset, Mater.Sci.Eng. B 12(1992) 281.
[2] J.Swenson, LBorjesson, Phys.Rev. B 57(21) (1998) 13514.
[3] M.Wollenhaupt, H.Ahrens, P.Frobel, K.Barner, E.Glessinger, R.Braunstein J.Non-Crys. Solids 194 (1996) 191.
[4] G.Ramadevudu, M.Shareefuddin, N.Sunitha Bai, M.Lakshmipathi Rao, M.Narasimha J.Non-Crys. Solids 278 (2000) 205.
[5] Mitsuru Kawashima, Yu Matsuda, Seiji Kojima J.Mol.Stru. 993(2011) 155-159.
[6] H.Hosono, Y.Abe, Solid State Ionics 44(1991) 293-297.
[7] H.Hosono, Y.Abe, J.American Ceramic Society 75(10)(1992) 2862-2864.
[8] B.K.Money, K.Hariharan, Applied Phys. A 88(2007) 647-652.
[9] X.Xu, Z.Wen, X.Yang,J.Zhang, Z.gu Solid State Ionics 177(2006) 2611-2615.
[10] R.C.Lucacel, M.Maier, V.Simon J.Non-Crys.Solids. 356(2010) 2869-2874.
[11] T.Y.Wei, Y.Hu, L.G.Hwa J.Non-Crys.Solids. 288(1-3)(2001) 140-147.
[12] H.R.Ahmadi Mooghari, Ali Nemathi, B.Eftekhari, Z.Hamnabard Ceramics Int. 38(2012) 3281-3290.
[13] Elias Oliverira Serqueira,Rodrigo Ferreira de Morais, Noelio Olivera Dantas J.alloys and Comp. 560(2013) 200-207.
[14] M.S.Gaafar, H.A.Afifi, M.M.Mekawy Physica B 404(2009) 1668-1673.
[15] S.Shailajha, K.Geetha, P.Vasantharani, S.P.Sheik Abdul Kathar Spectrochemica Acta Part A: Molecular and Biomolecular Spectroscopy 138(2015) 846-856.
[16] A.Chahine, M.Et-tabirou, J.L.Pascal Materials Letters 58(2004) 2776-2780.
[17] B .Eraiah, M.G.Smitha, R.V.Anavekar J.Phys.chem.Solids 71(2010) 153-155.
[18] G.Rajkumar, S.Aravindan, V.Rajendran J.Non-Crys. Solids 356(2010) 1432-1438.
[19]A.V.Gayathri Devi, V.Rajendran, N.Rajendran Int.J.Engg.sci.& Tech. Vol.2(6) (2010) 2483-2490.
[20] R.Ezhil Pavai, C.Tirumal Int.J. of Recent Sci. Research. Vol4, Issue.11(2013) pp.1915- 1919.
[21] Khamirul Amin Matori, Mohd Hafiz Mohd Zaid, Sidek Hj. Abdul Aziz, Halimah Mohamed Kamari, Zaidan Abdul Wahab J. Non-Crys.Solids. 361(2013) 78-81.
[22] Armando Mandule, Franziska Dohler, Leo Van Wullen, Toshihiro Kasuga, Delia S.Brauer J.non-Crys.Solids. 392-393(2014) 31-38.
[23] M.S.Gaafar, I.Shaarany, T.Alharbi J.Alloys & Compounds. (2014)
[24] K.Rao Structural Chemistry of Glasses, Elsevier, North Holland (2002).
[25] S.V Pakade, S.P.Yawale J.Pure & App.Ultrasonics Vol.18 (1996) P.74.
[26] A.N.Kannappan, S.Tirumaran, R.Palani ARPN J.Engg. & App.Sci. Vol.4 No.1(2009) ISSN 1819-6608.
[27] H.Sinouh, L.Bih, A.El Bouari, M.Azrour, B.Manoun, P.Lazor J.Non-Crys. Solids 405(2014) 33-38.
[28] Simon Striepe, Morten M.Smedskjaer, Joachim Deubener, Ute Bauer, Harald Behrens, Marcel Potuzak, John C.Mauro, Yuanzhen Yue, J.Non-Crys. Solids 364(2013) 44-52.
[29] R.Laopaiboon, C.Bootjomchai, M.chanphet, J.Laopaiboon Annals of Nuclear Energy 38(2011) 2333-2337.